Ivan ZAGRADIŠNIK[1], Miralem HADŽISELIMOVIĆ[1], Mitja HRIBERNIK[1], Tine MARČIČ[2]

University of Maribor, Faculty of Electrical Engineering and Computer Science (1),
TECES, Research and Development centre for Electric Machines (2)

Double fourier spectrum of air-gap magnetic field of outer-rotor single-phase induction motor

Abstract. *The paper presents the procedure for adequately obtaining the air-gap magnetic flux density spectrum by employing numerical field calculation using FEM and single (space field analyses) or double Fourier analyses (space and time field analyses). The double Fourier analysis is proven to be a helpful tool in analysing single-phase induction motors, where the excitation is explicitly time dependent. The problem of choosing adequate combinations of stator and rotor slots, and skewing is discussed. Specific results are presented for the 24/34 and 24/30 slot combination.*

Streszczenie. *W artykule przedstawiono procedurę wyznaczania spectrum strumienia magnetycznego w szczelinie powietrznej przy użyciu metody elementów skończonych połączonej z pojedyńczą (analiza przestrzenna) lub podwójną (analiza czasowo-przestrzenna) analizą fourierowską. Podwójna analiza Fouriera wykazała zasadność jej stosowania w analizowaniu jednofazowych silników indukcyjnych, gdzie wzbudzenie jest* explicite *czasowo-zmienne. Problem doboru właściwej kombinacji żłobków stojana i wirnika i ich skosów jest dyskutowany w artykule. Obliczenia zostały przeprowadzone dla kombinacji liczby żłobków 24/34 i 24/30.* ***(Podwójne widmo Fouriera pola magnetycznego w szczelinie powietrznej jednofazowego silnika indukcyjnego z zewnętrznym wirnikiem)***

Keywords: Double Fourier spectrum, finite element method, single-phase induction motors,.
Słowa kluczowe: podwójne widmo Fouriera, metoda elementów skończonych, silniki indukcyjne jednofazowe

Introduction

Experience has shown that the greatest costs for tools during the manufacture of a family of small power induction motors with outer rotor for direct drive of fans are the tools for punching stator and rotor laminations. Therefore it is common and especially for small series of such electric motors, that only one punching tool is used for the whole family of the same rotor outer diameter and for different three- and single-phase motor versions, i.e. motors with different ratings and different performance characteristics. In order to achieve different required target motor characteristics for ventilator fan drives, different stack lengths and also different rotor squirrel-cage die-casting material such as aluminium or its alloys aluminium-silicium, as well different squirrel-cage end-ring heights are employed. Additionally, capacitors of different capacitance are also used in single-phase motors [1-3]. In such a way, we can get a broad assortment of motors with different characteristics and which are produced with the same stator and rotor lamination.

Furthermore, such motors may be often supplied by triacs. In this case special care has to be taken regarding the common noise level of the fan and motor. This is directly connected with adequately choosing the number of stator and rotor slots [4-6], and especially in single-phase motors also the skewing angle [7] of the squirrel-cage. The choice depends on the motor size i.e. outer rotor diameter, which also influences the magnetic saturation of different parts in the motor's magnetic circuit and therefore it influences the motor's noise level.

Description of motors and their performance

In this paper, the selection procedure in accordance with analytical and numerical calculation results for the family of motors is presented. Table 1 presents design relevant data for the 4-pole three-phase motors and single-phase capacitor-run motors with rotor outer diameter of 102 mm (IEC size 71) and 24/34 (stator/rotor) slots combination. The second last row with one asterisk (*) in Table 1 presents data for the standard single-phase capacitor motor, and the last row with two asterisks (**) presents data for the newly proposed combination of 24/30 slots.

These kind of small four-pole motors with outer rotor for direct ventilator drives have usually 24 stator slots. The rotor can have different slot numbers, i.e. 28, 30, 32, and 34. Table 2 presents the motor's rated data for the motor with the 24/34 slot combination. Fig. 1a) and 1b) present the used stator and rotor slot shape. The focus of this analysis is on the single-phase motors because they are more problematic from the view of their noise level in comparison to three-phase motors.

Table 1. Overview of the family of induction motors used for ventilator drives

Induction motor	Stack length (mm)	Output power (W)	Rotor speed (rpm)	End-ring (mm)	Material	Cap. (μF)
3-phase	51	160	1330	19,5	AlSi12	-
3-phase	51	187	1330	2	Al	-
1-phase	51	87	1330	19,5	AlSi12	5
1-phase	51	137	1330	19,5	AlSi12	6,3
1-phase	51	173	1330	2	Al	6,3
3-phase	57	199	1400	15	Al	-
1-phase*	57	106	1400	19,5	AlSi12	6,3
1-phase**	57	106	1400	19,5	AlSi12	6,3

Table 2. Rated data of the single-phase motor

$P_s = 215$ W	$P = 106$ W
$U = 230$ V	$I = 1{,}15$ A
$\cos\varphi = 0{,}76$	$n = 1400$ min^{-1}
1 – phase	*freq.*: 50 Hz
Running capacitor: 6,3 μF, *U*: 450 V	

Table 3 presents an overview of the calculated electromechanical characteristics of the single-phase capacitor-run motor with 106 W output power by employing the existing slot combination (24/34 slots) and for the new 24/32, 24/30 and 24/28 slot combinations. The relatively high number of existing rotor slots (34) causes that the thickness of the rotor teeth is between 2,5 and 3,0 mm. Such narrow teeth are greatly influenced of by manufacturing technology, because the punching process damages the crystal structure of iron at the edge [8], and consequently increases the magnetizing current and losses of the motor. Laminations with higher number of slots have

teeth with smaller width and are therefore more affected by punching effects compared to laminations with small number of slots [9].

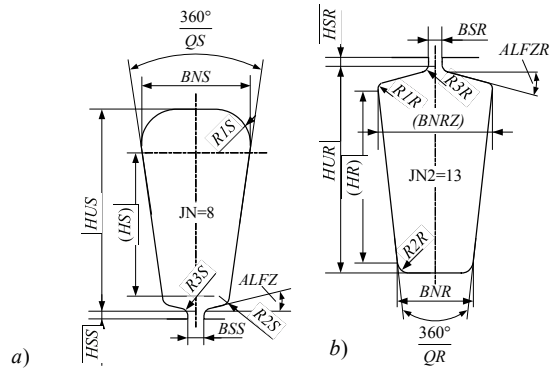

Fig.1. Stator slot a) and rotor slot b)

Table 3. Calculated performance data of the single-phase motor

No. of rotor slots	Input power (W)	Current (A)	Power factor	Rotor speed (rpm)
34	199,9	1,14	0,759	1418
32	199,6	1,14	0,759	1419
30	200,1	1,15	0,756	1420
28	202,5	1,16	0,753	1415

Numerical procedure, results and discussion

For the above stated reasons the goal of this study was to reduce the number of rotor slots and at the same time not to degrade the motor's performance. In ventilator drives the motor's rotational speed at rated load is one of the most important characteristics because the ventilator fan efficiency is optimised for one rotational speed and of course the motor's rotor speed has to correspond to it.

In order to choose the most adequate rotor slot number a detailed examination of the magnetic field in the motor's air-gap is necessary. Here the magnetic field computation by means of finite element method (FEM) and an analysis of harmonic spectrum of the air-gap's magnetic field provides information for choosing an adequate rotor slot number and also an adequate skewing of the rotor' squirrel-cage.

Computer software programs for analytical calculations, like "emLook" [10] which was used in obtaining the results in the previous section, enable quite accurate determination of three-phase and single-phase motor performance characteristics. However the analytical calculations do not enable the calculation of the harmonic spectrum of the air-gap field of the motor. The latter is a deciding factor for the noise level of the motor. In accordance, it is necessary to employ numerical field calculation by utilizing FEM. For three-phase motors the numerical field calculation does not present a problem. However, the case is different with single-phase capacitor-run motors. Fig. 2 shows the stator winding of such a four-pole single-phase motor with 24 stator slots. Fig. 3 shows, that the excitation in single-phase motors is time dependent, i.e. whether the main phase (MP) is the exciting one or the auxiliary phase (AP) is the exciting one or that both excite the field at the same time for a given moment in time. Therefore, the field has an elliptical shape (Fig. 4), i.e. time dependent, and the harmonic spectrum in the air-gap is changing with time.

Fig. 5 presents the air-gap magnetic flux density for the 24/34 slot combination plotted for ωt=0°, and Table 4 together with Fig. 6 show its corresponding harmonic spectrum (only harmonic components greater than 1,5 % of fundamental harmonic are presented). Table 5 together with Fig. 7 present the results for the 24/30 slot combination. In Tables 4 and 5 the total harmonic distortion factor THD without and with multiplication by the skewing factor is shown in the last row. The skewing was equal for all slot combination, i.e. 1/19 of the circumference or 360°/19. Based on the previously obtained results, one can decide which would be the adequate skewing angle for the rotor squirrel cage in question.

Here the question is how to choose the proper skewing of the rotor in order to reduce high order harmonics. And the answer is to calculate the magnetic field at the different time moments from 0 to 180 degree. And for correct results treatment of the numerical analyses of the air-gap field, the double Fourier analyses, i.e. the space and time field analyses [11] has to be employed; thus the double Fourier field spectrum is obtained.

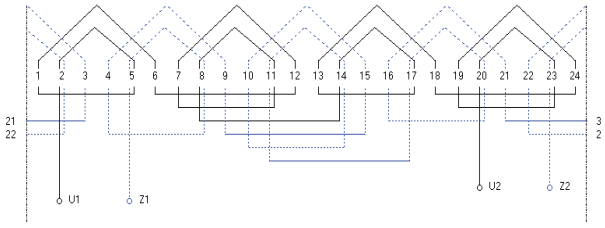

Fig.2. 4-pole single-phase stator winding on 24 slots

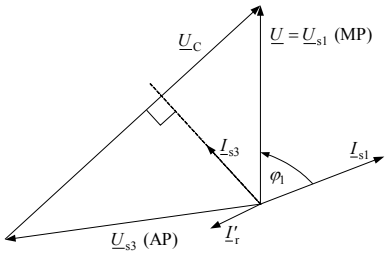

Fig.3. Phasor diagram of currents and voltages

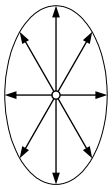

Fig.4. Elliptical magnetic field of fundamental harmonic

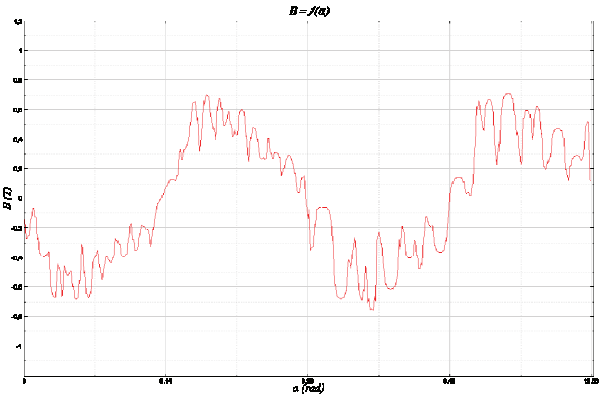

Fig.5. Fourier spectrum of air-gap field calculated at ωt=0° (24/34 slots)

Table 4. Fourier spectrum of air-gap field calculated at ωt=0° (24/34 slots)

Harm. order	B_d (T)	B_{dr} (%)	φ (rad.)	Skewing	B_d×Skew (%)
1	0,559	100,0	-1,754	0,982	100,0
3	0,092	16,5	-0,772	0,844	14,2
5	0,017	3,0	-0,847	0,603	1,9
7	0,015	2,7	2,414	0,318	0,9
9	0,019	3,4	2,698	0,055	0,2
11	0,028	4,8	-2,782	-0,131	-0,6
21	0,016	2,8	-2.240	0,088	0,3
23	0,068	12,2	-1,450	0,127	1,6
25	0,026	4,6	1,241	0,111	0,5
31	0,009	1,5	-1,935	-0,072	-0,1
33	0,012	2,1	-1,583	-0,091	-0,2
35	0,023	4,1	1,459	-0,072	-0,3
47	0,009	1,7	-1,637	0,011	0,0
		THD_B= 25,9			**THD×Skew= 14,56**

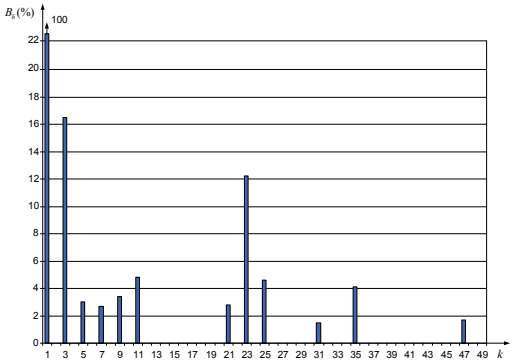

Fig.6. Fourier spectrum of air-gap field calculated at ωt=0° (24/34 slots)

Table 5. Fourier spectrum of air-gap field calculated at ωt=0° (24/30 slots)

Harm. order	B_d (T)	B_{dr} (%)	φ (rad.)	Skewing	B_d×Skew (%)
1	0,558	100,0	-1,747	0.982	100,0
3	0,089	15,9	-0,832	0,844	13,7
5	0,016	2,8	-0,833	0,603	1,7
7	0,012	2,2	2,649	0,318	0,7
9	0,021	3,7	2, 705	0,055	0,2
11	0,026	4,7	-2, 953	-0,131	-0,6
21	0,015	2,7	-2. 241	0,088	0,2
23	0,071	12,7	-1,475	0,127	1,6
25	0,026	4,7	1,323	0,111	0,5
29	0,014	2,4	-1,669	-0,017	-0,0
31	0,021	3,8	1,280	-0,072	-0,3
47	0,012	2,1	-1,594	0,011	0,0
49	0,013	2,2	1,023	-0,029	-0,1
		THD_B= 26,25			**THD×Skew= 14,08**

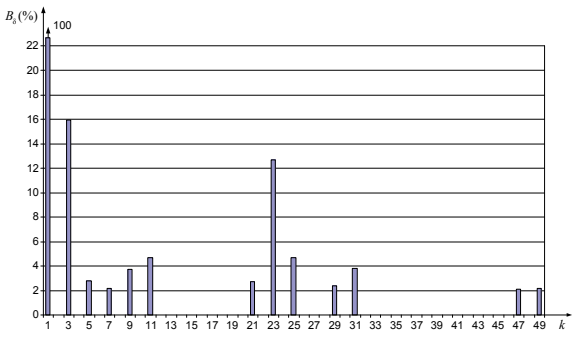

Fig.7. Fourier spectrum of air-gap field calculated at ωt=0° (24/30 slots)

Because of more and less elliptical magnetic field of fundamental harmonic (Fig. 4) in the air-gap of single-phase capacitor-run motors the time-stepping FE method has to be employed in the analysis. Time was changed from 0 to 179 degree by one degree, the time points from 180 to 360 degree are copied. There are 480 space points in the air-gap for two poles of four-pole motor. For Fourier analysis of the air-gap field the Bessel formulas were used. After the (first) space Fourier analysis, the air-gap field at any time point can be expressed as:

$$b(x,t) = \sum_{k=1}^{N-1} (B_{sk}(t)\sin(k\pi x/\tau_p) + B_{ck}(t)\cos(k\pi x/\tau_p)) \quad (1)$$

where "$2N$" is the number of space points and "k" is the number of space order ($k \le N$). The amplitude of the air-gap fundamental harmonic in the first row of Table 4 and 5 is equal.

$$B_{\delta k} = \sqrt{B_{sk}^2 + B_{ck}^2} \quad (2)$$

After the (second) time Fourier analysis of magnetic flux densities B_{sk} respectively B_{ck} and some mathematical arrangement the double Fourier spectrum of the air-gap field can be written as:

$$b(x,t) = \sum_{k=1}^{N-1}\sum_{\nu=1}^{M-1} (B_{k\nu p}\sin(k\pi x/\tau_p - \nu\omega_s t + \varphi_{k\nu p}) + B_{k\nu n}\sin(k\pi x/\tau_p + \nu\omega_s t + \varphi_{k\nu n})) \quad (3)$$

where "$2M$" is the number of time points in one period and "ν" is the number of time order ($\nu \le M$), "p" is positive and "n" is negative sequence component.

Fig. 8 shows the pulsation of air-gap field as results of double Fourier spectrum according to equation (3). Only the results of double Fourier spectrum give us the correct results of the air-gap field. By utilizing the double Fourier spectrum the results of positive and negative field components and their phase position according to winding on Fig. 2 are obtained (zero phase position is between slot 24 and 1). Results in Table 6 are presented for 24/34 slot combination and in Table 7 for the 24/30 combination. Presented are only the components greater then 1,5 % of the positive fundamental field component. From the presented results, it can be seen that both combinations of stator and rotor slots give approximately the same harmonic spectrum. For manufacturing reasons it is preferable to have 24/30 slots combination, i.e. less slots in the rotor.

Table 6. Air-gap field from double Fourier spectrum (24/34 slots)

Order		B_p (T)	φ_p (rad.)	B_n (T)	φ_n (rad.)
k	ν				
1	1	0,5694	-1,6787	0,0339	-2,8406
3	1	0,0205	-0,8502	0,0675	0,9900
5	1	0,0184	-1,3402	0,0053	-3,0384
7	1	0,0061	-2,0220	0,0136	-2,4752
9	1	0,0112	-0,3559	0,0084	-1,9976
11	1	0,0097	-2,2408	0,0185	-3,0380
21	1	0,0132	-2,4083	0,0031	3,1006
23	1	0,0076	-0,9412	0,0617	1,8767
25	1	0,0316	1,0310	0,0033	2,1668
33	1	0,0065	1,0817	0,0173	2,1190
35	1	0,0194	0,9228	0,0046	1,5881
1	3	0,0058	-0,0206	0,0058	1,6869
5	3	0,0087	-1,2844	0,0018	3,0456
5	5	0,0131	1,1603	0,0012	-0,0290

Table 7. Air-gap field from double Fourier spectrum (24/30 slots)

Order		B_p (T)	φ_p (rad.)	B_n (T)	φ_n (rad.)
k	ν				
1	1	0,5681	-1,6815	0,0324	-2,8693
3	1	0,0186	-0,8859	0,0653	1,0110
5	1	0,0197	-1,3866	0,0059	-2,8296
7	1	0,0082	-2,0230	0,0123	-2,5761
9	1	0,0130	-0,6498	0,0064	-2,1712
11	1	0,0068	-2,5379	0,0188	-3,0175
21	1	0,0131	-2,4394	0,0027	-2,6245
23	1	0,0081	-1,0564	0,0649	1,9040
25	1	0,0323	0,9984	0,0040	2,2854
29	1	0,0016	1,2781	0,0015	2,0960
31	1	0,0160	0,9007	0,0046	-1,0052
47	1	0,0017	-1,3926	0,0094	2,4590
49	1	0,0112	0,4487	0,0008	-1,2576
1	3	0,0200	-0,0184	0,0076	1,5822
5	3	0,0135	1,1840	0,0014	0,2683

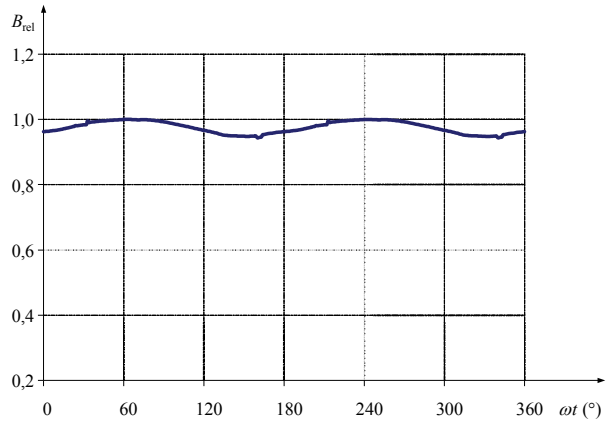

Fig.8. Pulsation of first order (fundamental harmonic) of air-gap field (24/34 slots)

Conclusion

The paper presents a detailed view of the family of small single-phase capacitor-run induction motors used for ventilator fan drives where the common noise level is very important. The motor's noise level depends on its air-gap magnetic flux density harmonic spectrum. Analytical calculation results of such small motors are not enough to determine the best suitable lamination. The presented procedure employing numerical field calculation by FEM and air-gap field analyses of single or double Fourier spectrum of the analysed motors are proven to be helpful tools for choosing the adequate combinations of the stator and rotor slots and skewing factor.

REFERENCES

[1] Zagradišnik I., Marčič T., Hadžiselimović M., Analysis of Single-Phase Induction Motor with Permanent Split Capacitor and Closed Rotor Slots, *Przegląd Elektrotechniczny*, 82 (2006), No. 5, 33-35

[2] Zagradišnik I., Gajzer M., Influence of winding on space harmonics of single-phase induction motor with permanent-split capacitor, *Electrotechnical Review*, 69 (2002), No. 3-4, 175-180

[3] Zagradišnik I., Gajzer M., Analiza enofaznega motorja z obratovalnim kondenzatorjem, *Proceedings International Electrotechnical and Computer Science Conference (ERK) 2001, Portorož, Slovenia*, A:449-454

[4] Kim B.-T., Kwon B.-I., Park S.-C., Reduction of Electromagnetic Force Harmonics in Asynchronous Traction Motor by Adapting the Rotor Slot Number, *IEEE Trans. Magn.*, 35 (1999), No. 5, 3742-3744

[5] Kobayashi T., Tajima F., Ito M., Shibukawa S., Effects of Slot Combination on Acoustic Noise from Induction Motors, *IEEE Trans. Magn.,* 33 (1997), No. 2, 2101-2104

[6] Marčič T., Štumberger B., Štumberger G., Hadžiselimović M., Zagradišnik I., Comparison of electromechanical characteristics of three phase induction motors with different pole and slot number combinations, *Int. J. Appl. Electrom.,* 31 (2009), No. 3, 161-169

[7] McClay C. I., Williamson S., The variation of cage motor losses with skew, *IEEE Trans. Ind. Applicat.,* 36 (2000), No. 6, 1563-1570

[8] Kedous-Lebouc A., Cornut B., Perrier J. C., Manfe P., Chevalier T., Punching influence on magnetic properties of the stator teeth of an induction motor, *J. Magn. Magn. Mater.*, 254 (2003), 124-126

[9] Marčič T., Štumberger B., Štumberger G., Hadžiselimović M., Zagradišnik I., The impact of different stator and rotor slot number combinations on iron losses of a three-phase induction motor at no-load, *J. Magn. Magn. Mater.*, 320 (2008), e891-e895

[10] Slemnik B., Zagradišnik I., emLook software package, Maribor, 2008

[11] Zagradišnik I., Influence of Saturation on the Stator Current of Single-phase Capacitor-run Motors at No-load *Proceedings Evolution of Modern Aspects of Induction Machines, 1986, Torino, Italy,* 278-281

***Authors**: Full Prof. Dr. Ivan Zagradišnik, Assit. Prof. Dr. Miralem Hadžiselimović, Mitja Hribernik, University of Maribor, Faculty of Electrical Engineering and Computer Science, Smetanova ulica 17, SI-2000 Maribor, Slovenia;*
Dr. Tine Marčič, TECES, Pobreška cesta 20, SI-2000 Maribor, Slovenia;
E-mail: ivan.zagradisnik@uni-mb.si.